Photon statistics of a cavity-QED laser: A comment on the laser–phase-transition analogy

Perry R. Rice
Department of Physics, Miami University, Oxford, Ohio 45056

H. J. Carmichael
Department of Physics, Chemical Physics Institute, and Institute of Theoretical Science, University of Oregon, Eugene, Oregon 97403

(Received 6 July 1994)

We develop a birth-death model for a cavity-QED laser and analyze the dependence of the lasing threshold on the fraction, β, of spontaneous emission directed into the laser mode. We define threshold in terms of the Fano factor for the intracavity photon number. We emphasize the role of β as a parameter characterizing the "system size" and show that the concept of laser threshold is well-defined in the "thermodynamic" limit, $\beta^{-1} \to \infty$. An ideal cavity-QED laser operates far outside this limit and therefore, in contrast to a conventional laser, is not a threshold device. We present numerical results showing how this difference affects the noise properties of the device.

PACS number(s): 42.55.−f, 42.50.Lc, 05.70.Fh

I. INTRODUCTION

There has been increasing interest over recent years in ways of modifying the radiative properties of atoms by changing the boundary conditions for the electromagnetic field [1,2]. Purcell initiated the area of study, now known by the name cavity quantum electrodynamics (cavity QED). He realized that coupling a radiative transition to a resonant oscillator could increase, or enhance, the spontaneous emission rate of the transition [3]; in modern versions of the effect the resonant oscillator is a resonant mode of an electromagnetic cavity. Kleppner pointed out that the spontaneous emission rate could also be inhibited by placing an atom in a cavity that is shorter than half the transition wavelength, in which case no resonant cavity modes exist to carry the emitted photon [4]. The inhibition of spontaneous emission occurs for similar reasons in photonic band gap materials—materials having a dielectric constant with crystalline symmetry [5]. The first experimental observation of a modified spontaneous emission rate was performed by Drexhage, who monitored the fluorescence from a monomolecular layer of dye atoms placed on the surface of a mirror [6]. Subsequently, several experiments have confirmed Purcell's prediction of an enhanced spontaneous emission rate [7]. The possibility of inhibiting spontaneous emission has also been experimentally confirmed [8].

Enhancement or inhibition of the spontaneous emission rate modifies the width of the spontaneous emission spectrum. The shape of the spectrum may also be altered. If an atom is placed in a cavity with sufficiently high Q the spectrum may be split into a doublet—the so-called "vacuum" Rabi splitting [9]. This splitting was first observed for many atoms [10], and recently for one atom (on average), by Thompson, Rempe, and Kimble [11].

Another way to modify the electromagnetic environment of an atom is to shine broadband squeezed light onto the atom. Linewidth changes produced by squeezed light have been discussed theoretically for atoms in free space [12,13] and in cavities [14,15]. These changes have not, as yet, been demonstrated experimentally.

As a result of all this work, it is now widely recognized that the radiative lifetime of an atom is as much a property of its environment as its heredity (the type of atom it is), and attention has turned to applications of cavity-QED effects. One proposal concerns the development of lasers. A laser "turns on" when the round-trip gain is greater than the round-trip loss. As the gain increases, so does the rate of spontaneous emission into nonlasing modes (due to the increased number of excited-state atoms). Any reduction in this spontaneous emission rate lowers the pump power required to make the laser lase. It has been proposed, therefore, that inhibiting the spontaneous emission into modes other than the lasing mode could lower the threshold pump power in semiconductor lasers [16]. The rates of spontaneous emission into lasing and nonlasing modes are conventionally stated as fractions, β and $1 - \beta$, of the total spontaneous emission rate. According to a rate equation analysis, when $\beta = 1$ the mean photon number increases linearly with pump power; the threshold pump power apparently vanishes, giving rise to the name "thresholdless laser," or "zero-threshold laser" [16–18]. We will refer to devices approaching this ideal limit as cavity-QED lasers.

For a conventional semiconductor laser β is a number on the order of 10^{-5} [19]. For gas lasers, β may be as small as 10^{-8} [20–23]. A group at AT&T Bell Laboratories recently constructed microdisk semiconductor lasers with β values as high as 0.1 [24], and it has been proposed that cylindrical microcavities could be constructed with a β of 0.7 [25]. In atomic systems, β values in the range

0.3–0.5 have been achieved at optical frequencies [26,27], although lasing in these systems has not been reported. At microwave frequencies, β values very close to unity have been realized [28–31].

This paper concerns the statistical mechanics of cavity-QED lasers. It is organized around a discussion of the laser–phase-transition analogy [32–34] and the related issue of laser threshold. The existing literature on thresholdless lasing presents a confusing picture of what happens to laser threshold in the cavity-QED limit. For example, when describing their experiments with microcavity dye lasers, DeMartini and co-workers speak of a "zero-threshold laser," suggesting a conventional laser threshold translated down to zero pump power [35]. These authors carry over the standard laser–phase-transition analogy, describing the behavior in their system as "an order-disorder transition at an extremely high value of the critical temperature." Björk and Yamamoto, on the other hand, define a nonzero-threshold pump power even for $\beta = 1$. In place of the conventional definition, they propose the pump power at which the mean stimulated and spontaneous emission rates into the lasing mode are equal (equivalently when the intracavity photon number is equal to unity) [36–38]. Our view is that such ambiguity is unnecessary. The notion of a "threshold" is grounded in a recognizable physical process (a point to which the designers of nuclear reactors would no doubt attest). The small ambiguities of definition that arise from the lack of strict discontinuity in real systems need not be magnified to the level of confusion one encounters in descriptions of thresholdless lasing.

We recall the fact that in equilibrium statistical mechanics, phase transitions, and the associated thresholds, draw their rigorous definition from the thermodynamic limit. Starting from this view, it is not possible to extend the phase-transition analogy (and the notion of laser threshold) to cavity-QED lasers without first identifying how one will take the thermodynamic limit. There are many versions of the microscopic statistical theory of conventional lasers in existence [21,22,39–43]. We show that in this theory the "thermodynamic" limit may be expressed in the form $n_{sat} = \beta^{-1} \to \infty$, where n_{sat} is the saturation photon number [43]. It follows that cavity-QED lasers operate, by definition, far outside the "thermodynamic" limit; $\beta = 1$ is so far from this limit it is misleading to think of the ideal cavity-QED laser as a threshold device at all—it truly is a *thresholdless* device. The issue is not entirely semantic. The statistical properties of conventional laser light are strongly influenced by the phase-transition nature of the laser "turn on," which guarantees they follow a generic, or universal form. This form does not transfer, even approximately, to cavity-QED lasers. We illustrate this fact using a birth-death model invented as a generalization of the standard laser rate equations. To keep the treatment simple we deliberately avoid the mathematical detail of a full microscopic theory. A more thorough microscopic approach could be taken by extending models that have been used to study one-atom lasers [44].

In Sec. II we construct the birth-death master equation for a cavity-QED laser, building upon the familiar semiclassical and rate equation theories of the laser. We review some results from the statistical theory of conventional lasers in Sec. III, and apply them to the definition of laser threshold. We discuss the changes that take place in the cavity-QED limit (outside the "thermodynamic" limit). In Sec. IV we illustrate this discussion with results computed from the birth-death master equation. A summary of the work and its conclusions is given in Sec. V.

II. THREE LASER THEORIES

Laser theories may be developed with various levels of sophistication. The discussion of cavity-QED lasers has been carried out, for the most part, using rate equation theories [17,36]. In addressing the question of laser threshold it is helpful to begin at a lower level, with the semiclassical laser theory of Lamb [45]. We consider a single-mode theory based on a four-level homogeneously broadened gain medium. The lower level of the lasing transition is rapidly depleted so that to a good approximation it remains empty. The laser mode and lasing transition are assumed to be exactly resonant. Mathematically, the model is defined by the Maxwell-Bloch equations (in a frame rotating at the laser frequency):

$$\dot{\alpha} = -\kappa\alpha + gv, \tag{1a}$$

$$\dot{v} = -(\gamma_h/2)v + g\alpha N, \tag{1b}$$

$$\dot{N} = -\tilde{\gamma}N + \Gamma - g(\alpha v^* + \alpha^* v). \tag{1c}$$

α is the complex amplitude of the laser field (in photon-number units), N is the number of carriers (atoms in the upper level of the lasing transition), and v is the gain-medium polarization amplitude summed over all carriers; 2κ is the photon decay rate, $\tilde{\gamma}$ is the spontaneous emission rate to modes other than the laser mode, γ_h is the gain linewidth (full width at half-maximum), and g is the dipole coupling constant. The steady-state solutions to Eqs. (1a)–(1c) are given by

$$\alpha(\tilde{\lambda}\tilde{\beta}|\alpha|^2 + \tilde{\lambda} - \tilde{\beta}\tilde{P}) = 0, \tag{2a}$$

$$N = \tilde{P}/(1 + \tilde{\beta}|\alpha|^2), \qquad v = (2g/\gamma_h)\alpha N, \tag{2b}$$

where $\tilde{\lambda}$, $\tilde{P}$, and $\tilde{\beta}$ are dimensionless parameters:

$$\tilde{\lambda} = 2\kappa/\tilde{\gamma}, \qquad \tilde{P} = \Gamma/\tilde{\gamma}, \qquad \tilde{\beta} = 4g^2/\gamma_h\tilde{\gamma}. \tag{3}$$

In a semiconductor laser carrier-carrier scattering damps the polarization on a subpicosecond time scale. The polarization may therefore be adiabatically eliminated. Then Eqs. (1a)–(1c) are replaced by equivalent rate equations:

$$\tilde{\gamma}^{-1}\dot{n} = -\tilde{\lambda}n + \tilde{\beta}nN, \tag{4a}$$

$$\tilde{\gamma}^{-1}\dot{N} = -N + \tilde{P} - \tilde{\beta}nN, \tag{4b}$$

where $n = |\alpha|^2$ is the photon number.

The semiclassical theory has the status of a mean-field theory in statistical mechanics. It neglects fluctuations and provides the description of the laser approached by

the full quantum statistical theory in the "thermodynamic" limit. The theory is used in this role by DiGiorgio and Scully to compare with the Weiss molecular field theory for the ferromagnet and hence establish the laser–phase-transition analogy [Eqs. (7) and (10) in Ref. [32]]. Note that the order parameter in the laser–phase-transition analogy is the complex field amplitude α which enters the semiclassical theory, not the photon number n which appears in rate equation theories. This can be appreciated by observing that the symmetry-breaking transition in the laser example, analogous to the choice of a magnetization direction in the ferromagnet, is the adoption above threshold of a definite phase for the electric field. Of course, in practice, this phase diffuses due to fluctuations, giving the laser a nonzero linewidth. Thus the semiclassical theory is an approximate theory for real lasers, which do not strictly operate in the "thermodynamic" limit. It is nevertheless fundamental; it describes the "thermodynamics" of the laser.

The rate equation theory usually used to analyze cavity-QED lasers [17–19] is not, in this sense, fundamental. On the other hand, it is more accurate than the semiclassical theory, since it includes at least some effects of the fluctuations. The rate equation theory generalizes Eqs. (4a) and (4b) by including spontaneous emission into the laser mode. The formal calculation involves an adiabatic elimination similar to that used to derive Eqs. (4a) and (4b); it must be carried out, however, at the level of operator equations. Setting details aside, the final outcome is the replacement of the photon number n by $n+1$ in the stimulated emission term $\tilde{\beta}Nn$. Thus we arrive at the rate equations

$$\gamma^{-1}\dot{n} = -\lambda n + \beta n N + \beta N, \tag{5a}$$

$$\gamma^{-1}\dot{N} = -N + P - \beta n N, \tag{5b}$$

where

$$\gamma = \tilde{\gamma} + 4g^2/\gamma_h \tag{6}$$

and we have new dimensionless parameters:

$$\lambda = 2\kappa/\gamma, \qquad P = \Gamma/\gamma, \tag{7a}$$

and

$$\beta = 4g^2/\gamma_h\gamma = \frac{4g^2/\gamma_h}{\tilde{\gamma} + 4g^2/\gamma_h}; \tag{7b}$$

λ and P are the cavity decay rate and pumping rate, respectively, measured in units of the spontaneous emission rate; β is the branching ratio which specifies the fraction of spontaneous emission directed into the laser mode. The steady-state solutions to Eqs. (5a) and (5b) are

$$n = (2\lambda\beta)^{-1}\left[-(\lambda - \beta P) \pm \sqrt{(\lambda - \beta P)^2 + 4\lambda\beta^2 P}\right], \tag{8a}$$

$$N = P/(1 + \beta n). \tag{8b}$$

Since n cannot be negative, the positive sign is to be taken in front of the square root.

By including the spontaneous emission term, the rate equations (5a) and (5b) account, partially, for quantum fluctuations, as we see explicitly in the next section. They do not, however, constitute a statistical theory. The rate equations tell us about the intensity of the emitted light. They cannot, however, tell us what kind of light is emitted; they cannot tell us about the fluctuations in the photon number. In order to obtain this information we need a theory that deals with probabilities. The simplest probabilistic theory may be written down directly from a birth-death model invented to reproduce Eqs. (5a) and (5b). The model is illustrated schematically in Fig. 1. It is essentially a translation of Einstein rate equation theory into probabilistic language for a field with uncertain energy density proportional to n. The pumping is included in a form that produces Poisson fluctuations in the carrier number. Mathematically, the model is described by a master equation for the probability $p_{n,N}$ of finding n photons in the laser mode and N carriers:

$$\begin{aligned}\gamma^{-1}\dot{p}_{n,N} = &-\lambda[np_{n,N} - (n+1)p_{n+1,N}] - \beta[nNp_{n,N} - (n-1)(N+1)p_{n-1,N+1}] - \beta[Np_{n,N} - (N+1)p_{n-1,N+1}] \\ &+P[p_{n,N-1} - p_{n,N}] - (1-\beta)[Np_{n,N} - (N+1)p_{n,N+1}].\end{aligned} \tag{9}$$

From the master equation the average photon and carrier numbers satisfy

$$\gamma^{-1}\langle\dot{n}\rangle = -\lambda\langle n\rangle + \beta\langle nN\rangle + \beta\langle N\rangle\ , \tag{10a}$$

$$\gamma^{-1}\langle\dot{N}\rangle = -\langle N\rangle + P - \beta\langle nN\rangle. \tag{10b}$$

These reproduce the rate equations (5a) and (5b) if we make the factorization $\langle nN\rangle = \langle n\rangle\langle N\rangle$.

The model defined at the beginning of this section is designed to realize the features of the ideal $\beta = 1$ cavity-QED laser, the device which shows thresholdless lasing. A more general (and realistic) model of a semiconductor laser must include background absorption. In this case, the rate equations (5a) and (5b) are replaced by [17,36]

$$\gamma^{-1}\dot{n} = -\lambda n + \beta n(N - N_0) + \beta N, \tag{11a}$$

$$\gamma^{-1}\dot{N} = -N + P - \beta n(N - N_0), \tag{11b}$$

where N_0 is the carrier number at transparency. The corresponding master equation has the term $-\beta N_0[np_{n,N} - (n+1)p_{n+1,N-1}]$ added to the right-hand side of Eq. (9).

III. LASING THRESHOLD

The rate equation solutions for the steady-state photon number and carrier number [Eqs. (8a) and (8b)] are plotted in Fig. 2 as a function of the pump parameter P for various values of β, reproducing the results of previ-

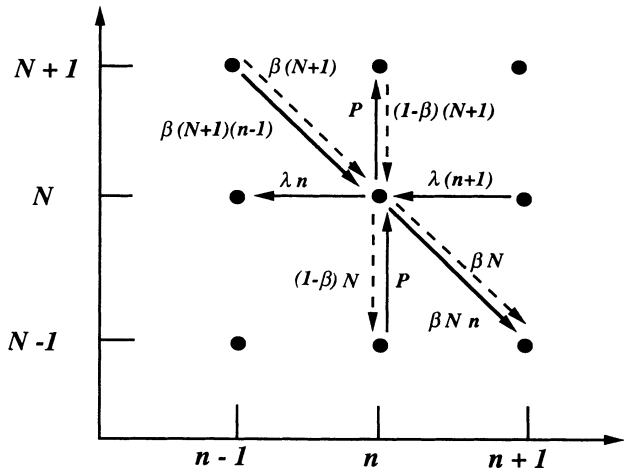

FIG. 1. Schematic representation of the birth-death process considered in the derivation of Eq. (9). The sketch shows the transition rates into and out of the state with photon number n and carrier number N.

ous authors [17–19,36,38]. With increasing β the curves approach the limiting results

$$n = P/\lambda, \qquad N = \lambda P/(\lambda + P). \tag{12}$$

Thus, when $\beta = 1$, the steady-state photon number increases monotonically with P.

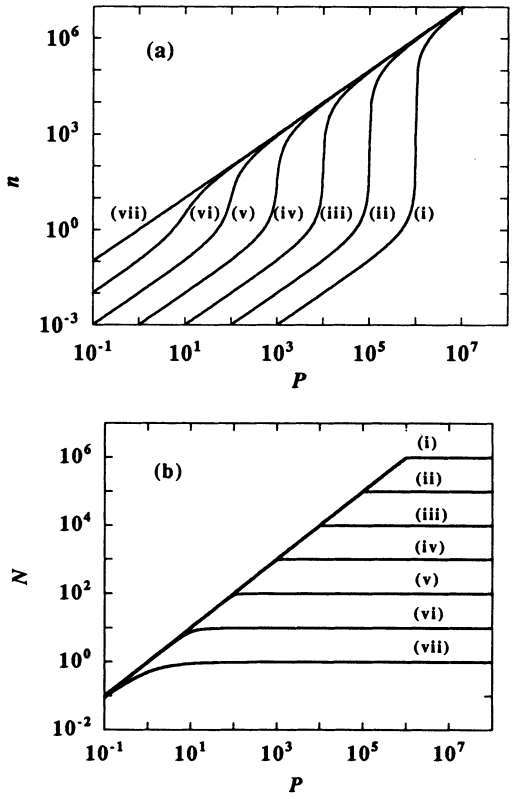

FIG. 2. Steady-state solutions to the rate equations (5a) and (5b) for $\lambda = 1$ and (i) $\beta = 10^{-6}$, (ii) $\beta = 10^{-5}$, (iii) $\beta = 10^{-4}$, (iv) $\beta = 10^{-3}$, (v) $\beta = 10^{-2}$, (vi) $\beta = 10^{-1}$, and (vii) $\beta = 1$.

Cavities with larger Q (lower λ) have larger slope efficiency, but not larger output power. In units of photons per atomic lifetime, the output power is given by the product of the photon number n and the dimensionless decay rate λ. Therefore, for $\beta = 1$ the output power is equal to P and exactly balances the input power.

For the typical β values of conventional semiconductor lasers ($\sim 10^{-5}$ [19]) there is a clear kink in the input-output curve which may be used to define laser threshold. The progression of the kink to lower pump powers with increasing β, culminating in its absence at $\beta = 1$, leads to the concept of thresholdless lasing. It is apparent from the figure, however, that as the location of the kink moves towards $P = 0$, it becomes less and less well-defined. It is not at all clear, therefore, that one can define a threshold all the way down to $P = 0$. Hence the confusing picture mentioned in the introduction:

(i) DeMartini and co-workers speak of a "zero-threshold laser" [35].

(ii) Björk and Yamamoto set the threshold pump power where the mean stimulated and spontaneous emission rates into the laser mode are equal [36–38].

(iii) Definitions of laser threshold based on kinks in other quantities, such as the variation of the degree of polarization with pump power, are also proposed [46].

To clarify the situation, in this section we discuss what the three theories introduced in Sec. II say about laser threshold. Our emphasis is on the importance of fluctuations, and we bring the statistical aspects out explicitly by using the Fano factor,

$$F = (\Delta n)^2/\langle n\rangle, \qquad (\Delta n)^2 = \langle n^2\rangle - \langle n\rangle^2, \tag{13}$$

as the signature of threshold behavior. The Fano factor defines a precise threshold pump power in the "thermodynamic" limit $\beta^{-1} \to \infty$, and a practically meaningful threshold when β^{-1} is large but not infinite. It shows also that the notion of laser threshold is meaningless when $\beta = 1$. In this conclusion we disagree with Jin *et al.*, who have recently proposed that the Fano factor always defines a finite threshold [47].

We begin the discussion by noting from Fig. 2 that as β increases, the kink defines threshold with fewer and fewer photons in the cavity and smaller and smaller numbers of carriers. Hence it would appear that, with increasing β, quantum fluctuations must play a larger and larger role. This conclusion follows in a more quantitative way from the equations. Equation (8b) gives the steady-state solution for the saturated carrier number N. This equation is central to the "thermodynamic" properties of the laser because it provides the nonlinearity which underlies the laser phase transition. From it we see that β^{-1} has the significance of a saturation photon number; we may rewrite Eq. (8b) as

$$N = \frac{P}{1 + n/n_{sat}}, \quad \text{with } n_{sat} = \beta^{-1}. \tag{14}$$

Even without a statistical analysis it is apparent from Eq. (14) that the saturation photon number determines

the importance of fluctuations. The saturation photon number provides the measure of "system size" which governs the scaling between extensive and intensive variables, hence determining the typical numbers of quanta present in the operating device. Thus it is the intensive variable

$$\bar{n} = n/n_{sat} = \beta n, \tag{15}$$

not the extensive variable n, which controls the gain saturation and the operating conditions of the laser above and around threshold (in the nonlinear regime). Stated another way, the nonlinearity which produces threshold behavior in a laser depends on the electromagnetic energy density seen by the gain medium, not on the total energy content of the laser mode. The importance of fluctuations then follows from the photon number needed to reach energy densities which "turn on" the nonlinearity. This number depends on n_{sat}. If n_{sat} is large (β is small) typical photon numbers are large and the relative fluctuations are small; if n_{sat} is small (β is large) typical photon numbers are small and the relative fluctuations large.

From these observations we see that the cavity-QED limit, $\beta \to 1$, is unavoidably tied to increased quantum fluctuations; the limit moves in the opposite direction to the "thermodynamic" limit, $n_{sat} = \beta^{-1} \to \infty$. The larger fluctuations convert the "thermodynamic," threshold behavior of conventional lasers, into a smooth, thresholdless evolution in the properties of a nonlinear noise process. Unexpected noise properties may arise as demonstrated in the cavity-QED limits of optical bistability [48–51] and parametric oscillation [52].

The argument based on Eq. (14) is a qualitative one. For something more quantitative we must turn to the full quantum statistical theory. For conventional lasers there are many versions of this theory in existence [21,22,39–43], and there is no need to reproduce their detail here. We simply review how the simple theories of Sec. II are tied together by the quantum statistical approach.

Quantum statistical treatments of the laser fall into two categories: phase-space treatments, which aim at a description in terms of a Fokker-Planck equation [21,22,41–43], and treatments built around density matrix equations [39,40]. The phase-space approach is more suitable for our purpose because it gives a clear view of the "thermodynamic" limit. The theory assumes that n_{sat} is large (β is small) and establishes the "thermodynamic" equations underlying the laser–phase-transition analogy in the limit $n_{sat} = \beta^{-1} \to \infty$. The assumption of a large saturation photon number justifies a perturbative calculation: a linearization of fluctuations below threshold, lowest-order nonlinear treatment of fluctuations at threshold, and quasilinearization above threshold. Technically, an expansion is performed in inverse powers of n_{sat}. By this device a separation is made between a set of "thermodynamic," or mean-value equations describing nonlinear deterministic physics, and a Fokker-Planck equation which describes small (on the scale of n_{sat}) fluctuations about the mean.

The "thermodynamic" equations are those of the semiclassical theory [Eqs. (1a)–(1c)]. These equations yield the most commonly quoted definition of laser threshold. The definition follows from Eq. (2a), which has two solutions for the steady-state photon-number density:

$$\bar{n} = 0 \quad \text{and} \quad \bar{n} = (1-\beta)(\tilde{P}/\tilde{P}^{sc}_{thr} - 1), \tag{16}$$

where the second solution holds above the threshold pump power

$$\tilde{P}^{sc}_{thr} = \tilde{\lambda}/\tilde{\beta} = \lambda/\beta. \tag{17a}$$

We may write Eq. (17a) in the alternative form

$$P^{sc}_{thr} = (1-\beta)P_{thr}, \tag{17b}$$

where

$$P_{thr} = \lambda/\beta; \tag{18}$$

note that $P^{sc}_{thr} \to P_{thr}$ in the "thermodynamic" limit. At the semiclassical threshold the round-trip stimulated emission gain is equal to the round-trip loss. Above threshold, the gain exceeds the loss and the solution $\bar{n} = 0$ becomes unstable. Thus in the "thermodynamic" limit there is a single stable steady-state solution for the photon-number density. The solution changes continuously as a function of P with discontinuous slope at $P/P_{thr} = 1$.

Equation (17b) provides the reason for speaking of a "zero-threshold" laser when $\beta = 1$ [35]. It is derived, however, from "thermodynamic" equations, and there is no justification for applying it outside the "thermodynamic" limit.

Superficially, the rate equations (5a) and (5b) completely change the picture of laser threshold. They give one positive solution for n which varies continuously as a function of P with *continuous* slope [Eq. (8a)]. We must remember, however, that these equations are not "thermodynamic" equations. They do, on the other hand, contain the "thermodynamic" limit. If we rewrite Eq. (8a) as

$$\bar{n} = \tfrac{1}{2}\left[-(1-P/P_{thr}) \pm\sqrt{(1-P/P_{thr})^2 + 4\beta P/P_{thr}}\right], \tag{19}$$

we may take the "thermodynamic" limit in the form $\beta \to 0$, $\lambda \to 0$, with $P_{thr} = \lambda/\beta$ finite. In this way we recover the semiclassical solutions (16) (for $\beta \to 0$).

Outside the "thermodynamic" limit, Eq. (19) gives corrections due to fluctuations. Thus, at the "thermodynamic" threshold, $P/P_{thr} = 1$, we find

$$\bar{n}_{thr} = \beta^{1/2}; \tag{20}$$

expanding the square root to lowest order, below and above, but not too close to threshold ($|P/P_{thr} - 1| \gg \beta^{1/2} = n_{sat}^{-1/2}$), we find

$$\bar{n}_{<} = \beta\frac{P/P_{thr}}{1-P/P_{thr}}, \tag{21a}$$

$$\bar{n}_> = (P/P_{thr} - 1) + \beta \frac{P/P_{thr}}{P/P_{thr} - 1}. \quad (21b)$$

It follows from Eqs. (15) and (20) that $n_{thr} = \beta^{-1/2}$, a number much larger than unity in a conventional laser. The notion that the laser "turns on" when the rate of stimulated emission exceeds the rate of spontaneous emission is therefore clearly a misnomer. From Eq. (21a), the stimulated emission rate already greatly exceeds the spontaneous emission rate below threshold, the rates being equal at the pump power

$$P_{n=1} = P_{thr}(1 + \beta)/2, \quad (22)$$

one-half the threshold pump power in the "thermodynamic" limit. A more accurate description is that the turning on of the laser is caused by an explosion of stimulated emission, an explosion held in check below threshold by the cavity loss. Since the photon number increases smoothly with P, it is important to consider the intensive variable $\bar{n}$ in the "thermodynamic" limit in order to recognize the explosion. In the "thermodynamic" limit $\bar{n}$ is zero for $P/P_{thr} < 1$; it is also zero for $P/P_{thr} = 1$, even though n is now infinite [Eq. (20)]. For $P/P_{thr} > 1$, $\bar{n}$ becomes nonzero [Eq. (21b)]. This is the explosion.

For $\beta = 1$, Eq. (22) gives $P_{n=1} = P_{thr}$. This provides a rationale for the position of Yamamoto and coworkers, who define the threshold pump power of cavity-QED lasers by the condition that the mean stimulated and spontaneous emission rates into the laser mode are equal [36–38]. The position has two arguments against it, however. As noted, the "thermodynamic" threshold occurs at twice the pump power defined by the condition of Yamamoto and co-workers; also, as before, the proposal arbitrarily extrapolates a "thermodynamic" concept far outside the "thermodynamic" limit.

We have now seen how the rate equations (5a) and (5b) are connected to the "thermodynamic" laser equations. What is their connection to the full quantum statistical theory, including fluctuations? As was noted in Sec. II, adding spontaneous emission at the level of rate equations gives only a partial account of the fluctuations. Some of the results we have derived from Eq. (19) are not, therefore, correct. More important for our purposes is the fact that the rate equation theory provides no information about the photon-number variance. The behavior of this quantity as a function of P/P_{thr} provides a particularly clear view of the threshold region and how it changes with β.

The results we now quote were obtained from the phase-space version of the quantum statistical theory [53]. They could be reproduced, however, from the birth-death master equation (9).

In place of Eqs. (20)–(21b), the full quantum statistical theory gives

$$\bar{n}_{thr} = \beta^{1/2}\sqrt{2/\pi}, \quad (23)$$

and

$$\bar{n}_< = \beta \frac{P/P_{thr}}{1 - P/P_{thr}}, \quad (24a)$$

$$\bar{n}_> = (P/P_{thr} - 1) + \beta \frac{1}{4} \frac{1}{P/P_{thr} - 1} \frac{P/P_{thr} + 1}{2P/P_{thr}}. \quad (24b)$$

Compared with the rate equation results, in these expressions the photon number at threshold is smaller by a factor $\sqrt{2/\pi}$, and above threshold the incoherent contribution $\bar{n}_> - (P/P_{thr} - 1)$ is smaller by a factor 1/4. To characterize the photon-number fluctuations we calculate the Fano factor [Eq. (13)]. The quantum statistical theory gives the following results: at the "thermodynamic" threshold, $P/P_{thr} = 1$,

$$F_{thr} = \beta^{-1/2}\left(\sqrt{\pi/2} - \sqrt{2/\pi}\right); \quad (25)$$

below and above, but not too close to threshold ($|P/P_{thr} - 1| \gg \beta^{1/2} = n_{sat}^{-1/2}$),

$$F_< = 1 + \frac{P/P_{thr}}{1 - P/P_{thr}}, \quad (26a)$$

$$F_> = 1 + \frac{1}{P/P_{thr} - 1} \frac{P/P_{thr} + 1}{2P/P_{thr}}. \quad (26b)$$

The behavior of the Fano factor as a function of pump power is illustrated schematically in Fig. 3. In the "thermodynamic" limit it shows a singularity at threshold: well below threshold, where the field is in a weakly excited thermal state, $F_< = 1$; well above threshold, where the field is in a coherent state, $F_> = 1$; at threshold, $F \to \infty$. Conventional lasers do not strictly operate in the "thermodynamic" limit. Nevertheless, with $\beta \sim 10^{-5} - 10^{-8}$ ($n_{sat} \sim 10^5 - 10^8$) the Fano factor shows a well-localized peak in the vicinity of the "thermodynamic" threshold. In practical terms, a threshold pump power can still be defined with a relative precision of at least a few tenths of a percent. If, however, we extrapolate the $\beta^{1/2}$ peak width to $\beta = 1$, the notion of a threshold pump power becomes meaningless; the uncertainty in locating P_{thr} becomes as large as P_{thr} itself; moreover, the sense of dramatic change (singular behavior) that is carried by the word "threshold" clearly no longer applies.

Figure 3 gives an unconventional view of laser thresh-

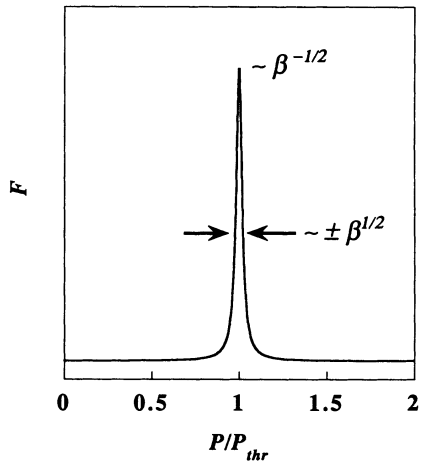

FIG. 3. Schematic variation of the Fano factor with pump power for a conventional laser (large n_{sat} and small β).

old. Historically, it has been the practice (with one or two exceptions [54]) to characterize the photon-number fluctuations by the reduced factorial moment $\langle n(n-1)\rangle/\langle n\rangle^2 - 1 = (F-1)/\langle n\rangle$ [20,22,55–57]. This quantity decreases monotonically through the threshold region, from unity below threshold to a number on the order of β^{-1} above. We use the Fano factor rather than the reduced factorial moment because it scales with system size in the same way as the fluctuations in the order parameter. As stated earlier, the order parameter in the laser–phase-transition analogy is the complex field amplitude $\bar{\alpha} = \alpha/n_{sat}^{1/2}$, not $\bar{n} = n/n_{sat}$. From the full quantum statistical theory, fluctuations in the order parameter scale below, at, and above threshold, according to the scheme [43]:

$$
\begin{aligned}
&|\Delta\bar{\alpha}|_< \sim \langle|\bar{\alpha}|\rangle_< \sim \beta^{1/2}, \\
&|\Delta\bar{\alpha}|_{thr} \sim \langle|\bar{\alpha}|\rangle_{thr} \sim \beta^{1/4}, \\
&(\Delta|\bar{\alpha}|)_> \sim \beta^{1/2} \text{ and } \langle|\bar{\alpha}|\rangle_> \sim 1.
\end{aligned}
\tag{27}
$$

Thus the fluctuations increase at threshold, by a factor of $\beta^{-1/4}$, and decrease again above threshold as the laser chooses a well-defined phase and the magnitude of the order parameter acquires a nonzero value. The photon-number fluctuations are related to the fluctuations in the order parameter by

$$
\begin{aligned}
&(\Delta\bar{n})_< \sim \langle\bar{n}\rangle_< \sim (|\Delta\bar{\alpha}|_<)^2 \sim \beta, \\
&(\Delta\bar{n})_{thr} \sim \langle\bar{n}\rangle_{thr} \sim (|\Delta\bar{\alpha}|_{thr})^2 \sim \beta^{1/2}, \\
&(\Delta\bar{n})_> \sim \langle|\bar{\alpha}|\rangle_>(\Delta|\bar{\alpha}|)_> \sim \beta^{1/2} \text{ and } \langle\bar{n}\rangle_> \sim 1.
\end{aligned}
\tag{28}
$$

Note that above threshold, $\bar{n}$ is calculated from $[\langle|\bar{\alpha}|\rangle_> + (\Delta|\bar{\alpha}|)_>]^2$. It follows from Eqs. (27) and (28) that βF scales in the same way as the square of the fluctuations in the order parameter.

The system size expansion is not valid for $\beta = 1$. We have therefore solved the birth-death master equation (9) numerically to illustrate what happens in the cavity-QED limit.

IV. NUMERICAL RESULTS

Since the birth-death master equation only reproduces the rate equations under a factorization assumption, it is not necessary that the exact averages for the steady-state photon number and carrier number agree with Eqs. (8a) and (8b). Figure 4 shows the behavior of these averages as a function of the pump power P for $\beta = 1$ and $\lambda = 1$. We see that the average photon number does agree with the rate equation result, but the average carrier number differs substantially throughout the saturation region; although it eventually saturates at the value given by the rate equations ($\langle N\rangle = \lambda = 1$). It is clear from Eqs. (10a) and (10b) why the average photon number agrees with the rate equation result. For $\beta = 1$, Eq. (10b) may be solved for $\langle N\rangle + \langle nN\rangle = P$; Eq. (10a) then gives $\langle n\rangle = P/\lambda$. The same procedure carries through

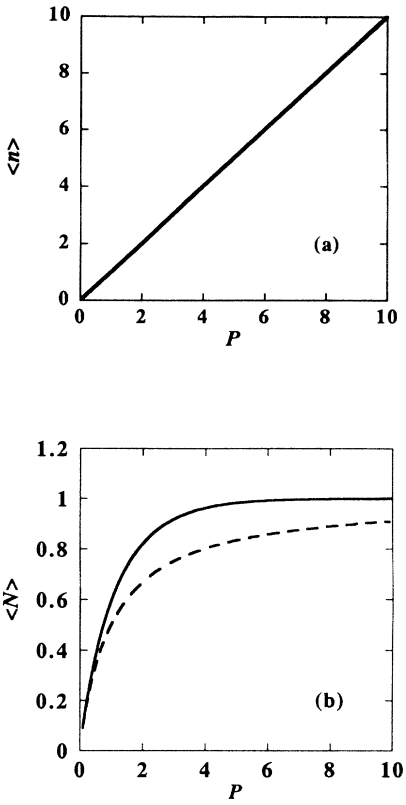

FIG. 4. Average photon and carrier numbers in the steady state as a function of pump power for $\beta = 1$ and $\lambda = 1$. The solid lines are the results obtained by numerical solution of the truncated birth-death process. The dashed lines are the rate equation results plotted from Eqs. (8a) and (8b). For the average photon number the two sets of results overlap.

whether or not the factorization $\langle nN\rangle \to \langle n\rangle\langle N\rangle$ is made. Of course, physically, the linear relationship $\langle n\rangle = P/\lambda$ must hold for energy to be conserved.

The disagreement for the average carrier number is an indication of the importance of fluctuations in the cavity-QED limit. More precisely, it indicates the importance of correlations between photon-number and carrier-number fluctuations—$\langle nN\rangle \neq \langle n\rangle\langle N\rangle$. Correlations exist because fluctuations on the scale of just one photon cause significant carrier saturation when $\beta = 1/n_{sat} = 1$; such fluctuations have no affect on the carrier number in the "thermodynamic" limit. Focusing on the fluctuations, in Fig. 5 we plot the photon-number distribution for various values of the pump power P. Qualitatively, the distribution undergoes a similar evolution with increasing pump power to that observed in the threshold region of a conventional laser [22,39,43,55,57,58]. The similarity is superficial, however, and does not amount to a translation of the conventional laser threshold to either $P = 0$ [35] or $P = 1$ [36–38]. Of the two suggestions, perhaps the second receives the stronger support from the figure. In a conventional laser, at threshold the photon-number distribution has zero slope at $n = 0$ [39,43]. The distributions plotted in Fig. 5 do evolve to the zero-slope form at some nonzero pump power. The condition is not met,

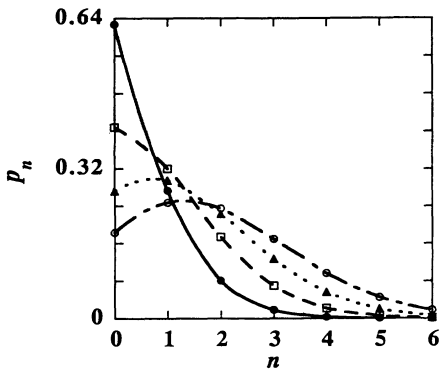

FIG. 5. Photon-number distribution for $\beta = 1$, $\lambda = 1$, and $P = 0.5$ (solid circles), $P = 1.0$ (squares), $P = 1.5$ (diamonds), and $P = 2.0$ (open circles).

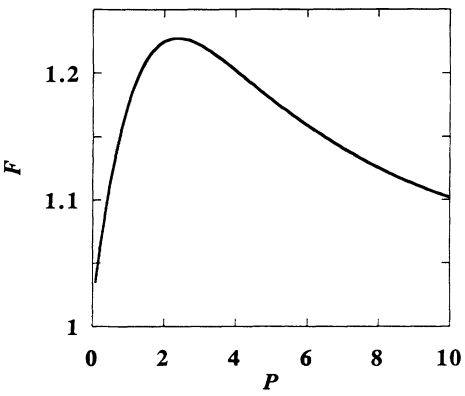

FIG. 6. Variation of the Fano factor with pump power for $\beta = 1$ and $\lambda = 1$.

however, at $P = 1$, but somewhere between $P = 1$ and $P = 1.5$. Moreover, there is nothing of the sudden change associated with a threshold phenomenon in Fig. 5; if, for the sake of argument, a "threshold" is defined to lie at $P = 1$, the change in the photon-number distribution is far less dramatic over a range extending from 100% below "threshold" to 100% above "threshold," than it is over a range within 0.1% of threshold in a conventional laser [59].

With more thought it is not even reasonable to favor a threshold at, or near, $P = 1$, over one at $P = 0$ on the basis of Fig. 5. Consider the possibility that the laser field is in a coherent state for all pump powers. The photon-number distribution is then a Poisson distribution, which evolves from a monotonically decreasing distribution to a peaked distribution, passing through a form with zero slope ($p_0 = p_1$) when $\langle n \rangle = 1$. For the parameters of Fig. 5, the zero slope condition would be met at $P = 1$; but there would clearly be no justification for speaking of a threshold at this pump power. The use of the zero-slope condition to locate threshold in a conventional laser relies on the fact that the mean photon number is large near threshold. Then something as simple as the slope at $n = 0$ can distinguish a Bose-Einstein distribution (below threshold) from a broadened Poisson distribution (above threshold).

All of these comments spring from the fact that the threshold concept becomes meaningless once the fluctuations about "thermodynamic" values, caused by a finite system size, are no longer confined to a well-defined transition region, as they are in Fig. 3. For comparison with Fig. 3 we plot the Fano factor as a function of pump power for a $\beta = 1$ cavity-QED laser in Fig. 6. A peak still exists, but it is very broad, and it rises a mere 20% above the background, a rather insignificant remnant of the divergence that occurs in the "thermodynamic" limit. The peak appears at $P \approx 2.5$. This is different from the pump power at which the photon-number distribution has zero slope at $n = 0$ (Fig. 5), and different again from the pump power at which the average photon number is equal to unity. In fact, the location, width, and height of this peak changes with the cavity decay rate λ. This is shown in Fig. 7, where we plot the Fano factor as a function of pump power for cavity decay rates that are ten times smaller and ten times larger than in Fig. 6. The peak position does not move in direct proportion to λ, as does the "thermodynamic" threshold. In Fig. 7, peaks appear at $P \approx 1.9\lambda$ and $P \approx 4.5\lambda$, both different from the position $P \approx 2.5\lambda$ in Fig. 6. The trend in the peak height, moving from larger to smaller values of λ, appears to be approaching a limit in which $F = 1$ for all pump powers. This good-cavity limit may be understood by making an adiabatic elimination in the master equation (9). For $\beta = 1$ and $\lambda \ll 1$, the pumping transitions (vertical arrows in Fig. 1) reach an equilibrium with the spontaneous and stimulated emission (diagonal

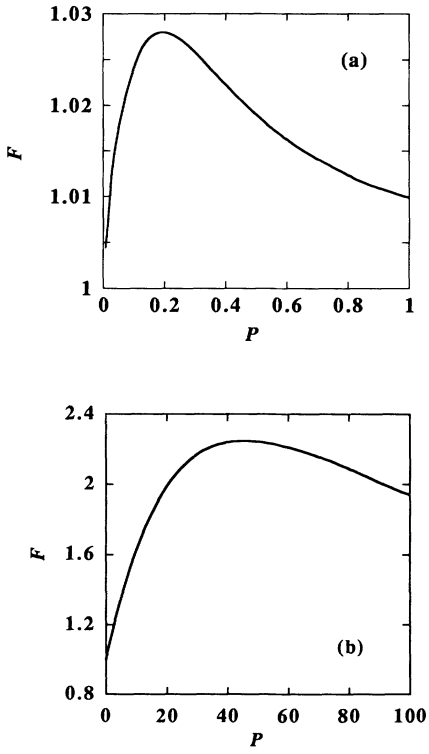

FIG. 7. Variation of the Fano factor with pump power for $\beta = 1$ and (a) $\lambda = 0.1$, (b) $\lambda = 10$.

arrows in Fig. 1) in a time much shorter than the cavity decay time. Then, setting

$$Pp_{n,N-1} = (n+1)Np_{n,N} \tag{29}$$

in Eq. (9), and summing over carrier numbers, we obtain the photon-number master equation

$$\gamma^{-1}\dot{p}_n = -\lambda[np_n - (n+1)p_{n+1}] + P(p_{n-1} - p_n). \tag{30}$$

Equation (30) describes a damped cavity mode pumped at the constant rate $\gamma P = \Gamma$. In steady-state it is solved by the Poisson distribution

$$p_n = \frac{(P/\lambda)^n}{n!}e^{-P/\lambda}. \tag{31}$$

Using Eq. (29), the full distribution, over photon and carrier numbers, is

$$p_{n,N} = p_n p_{N|n}, \tag{32}$$

where $p_{N|n}$ is the conditional distribution

$$p_{N|n} = \frac{[P/(n+1)]^N}{N!}e^{-P/(n+1)}. \tag{33}$$

Apparently the good-cavity limit produces the ideal thresholdless laser. Not only does the average photon number grow linearly with the pump power, the photon-number distribution is also a Poisson distribution. The appearance may be misleading, however. Without analyzing the phase fluctuations, we cannot conclude that the field is in a coherent state. Perhaps the direct pumping of the cavity mode randomizes the phase, in which case this good-cavity device produces light with the cavity linewidth; then, if it is a laser at all, it is a laser whose linewidth is dominated by a power-independent component [60].

Semiconductor lasers operate in the bad-cavity limit. Therefore the super-Poissonian statistics of Fig. 7(b) are more relevant to these devices than the Poisson limit suggested by Fig. 7(a). Typical values of λ are $\sim 10^3$ [36,38,47]. For λ as large as this, Figs. 7(a) and 7(b) could be extrapolated to a relatively high peak. Perhaps the Fano factor then reveals a well-defined transition region in a similar fashion to Fig. 3; but with an inverse power of λ acting as the small parameter in place of $\beta^{1/2}$. To check on this possibility it would be useful to have an approximate solution for the bad-cavity limit analogous to the good-cavity solution given by Eqs. (31)–(33). Unfortunately, we are not able to find such a solution unless $P/\lambda \ll 1$, and this restriction excludes the range of pump powers over which the Fano factor peaks. Some headway can be made, however, by working directly with the moment equations.

We have noted that for $\beta = 1$ the rate equation solution for the mean photon number is exact (Fig. 4); thus, from the equations for first-order moments [Eqs. (10a) and (10b)], we have

$$\langle n\rangle = n_r, \qquad \langle N\rangle = N_r - (\langle nN\rangle - n_r N_r), \tag{34}$$

where n_r and N_r are the quantities denoted by n and N in Eq. (12). We are able to solve for $\langle n\rangle$ exactly because only one moment other than $\langle n\rangle$ appears in Eqs. (10a) and (10b); moreover, this moment—$\langle(n+1)N\rangle$—enters both equations and can therefore be eliminated between them. A similar simplification occurs in the equations for second-order moments which enables us to derive a simple expression for the Fano factor. From the master equation (9) we obtain the moment equations ($\beta = 1$)

$$(2\gamma)^{-1}\frac{d}{dt}\langle n(n-1)\rangle = -\lambda\langle n(n-1)\rangle + \langle n(n+1)N\rangle, \tag{35a}$$

$$(2\gamma)^{-1}\frac{d}{dt}\langle N(N-1)\rangle = -\langle(n+1)N(N-1)\rangle + P\langle N\rangle, \tag{35b}$$

$$\gamma^{-1}\frac{d}{dt}\langle(n-1)N\rangle = -\lambda\langle nN\rangle + \langle(n+1)N(N-n)\rangle + P\langle n-1\rangle. \tag{35c}$$

Solving these equations in the steady state and using Eq. (34), we find the relationship

$$(F-1)/\lambda = \langle N\rangle/N_r - 1. \tag{36}$$

This does not provide an exact solution for the Fano factor since $\langle N\rangle$ is still undetermined. The dependence of F on λ can, however, be understood with the help of Eq. (36).

In the good-cavity limit, the distribution (32) gives

$$\langle N\rangle = \lambda(1 - e^{-P/\lambda}); \tag{37}$$

we then find ($\lambda \ll 1$)

$$(F-1)/\lambda = \frac{1+P/\lambda}{P/\lambda}(1 - e^{-P/\lambda}) - 1. \tag{38}$$

According to this expression $(F-1)/\lambda$ rises to a maximum, $(F-1)/\lambda \approx 0.3$, at $P/\lambda \approx 2$. For large P/λ, it approaches zero with $(F-1)/\lambda \sim \lambda/P$. This behavior agrees well with the numerical results of Fig. (7a) ($\lambda = 0.1$). The trend with increasing λ follows from Eq. (36). Numerical results show that $\langle N\rangle$ approaches N_r as λ increases. The approach is nonuniform with respect to the variable P/λ, proceeding most rapidly where the difference between $\langle N\rangle$ and N_r is largest. It follows that the peak in $(F-1)/\lambda$ becomes both smaller and broader as λ increases. The development is illustrated in Fig. 8.

Figure 8(b) shows that the peak in F actually grows rather slowly with increasing λ. At $\lambda = 10^2$, the maximum value of the Fano factor is $F_{max} \approx 6$. By plotting $\log F_{max}$ versus $\log\lambda$, for large λ it appears that $F_{max} \approx 0.6\lambda^{1/2}$. At $\lambda = 10^3$ this gives $F_{max} \approx 19$. We can also estimate how the width of the peak changes for large λ. Since $\langle N\rangle$ saturates faster than N_r [Fig. 8(a)], Eq. (36) tells us that $(F-1)/\lambda$ approaches zero asymptotically as λ/P. The peak therefore falls to half its maximum value when $F \sim \lambda^2/P \approx 0.3\lambda^{1/2}$. This condition gives a peak width, $(\Delta P)/\lambda \approx 3.3\lambda^{1/2}$. Finally, we estimate that the peak maximum occurs at a pump power slightly less than $P/\lambda = \frac{1}{2}(\Delta P)/\lambda \approx 1.6\lambda^{1/2}$. These es-

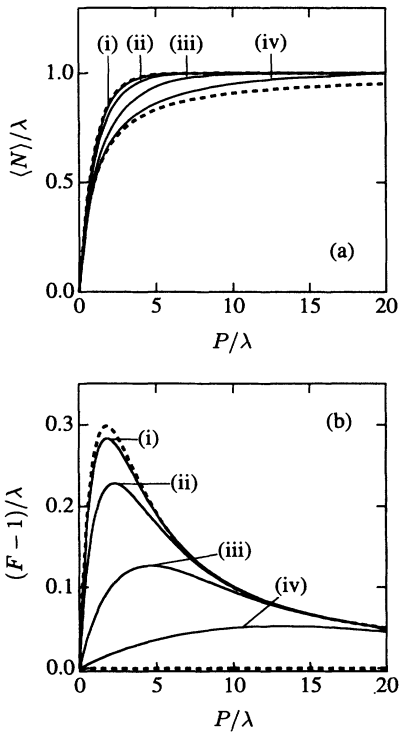

FIG. 8. Numerical results illustrating the relationship between the saturation of the average carrier number (a) and the peak in the Fano factor (b). The upper dashed lines are the bounds set by the good-cavity limit [Eqs. (37) and (38)]. The lower dashed lines are the bounds set by the rate equation approximation. The solid lines show numerical results for (i) $\lambda = 0.1$, (ii) $\lambda = 1$, (iii) $\lambda = 10$, and (iv) $\lambda = 100$.

timates may not be very accurate since we do not have numerical results for very large values of λ. It is clear, however, that there is no sharply defined transition region resembling that in Fig. 3. As λ increases the peak in the Fano factor becomes less, not more, well defined. Note also that for $\lambda \gg 1$ the maximum value of the Fano factor occurs when the mean photon number is quite large—$\langle n\rangle = P/\lambda \approx 1.6\lambda^{1/2}$; this is very far from the "threshold" at $\langle n\rangle = 1$ proposed by Yamamoto and coworkers [36–38].

The behavior we have described as a function of λ is different from that obtained by Jin *et al.*, who also calculated the Fano factor near the $\beta = 1$ limit [47]. The differences can be accounted for by differences in the underlying models. Jin *et al.* use a model in which the lower lasing level is a ground state. In this situation absorption from the populated ground state plays an important role. We have eliminated absorption, assuming that the lower laser level rapidly decays to a lower state (and setting $N_0 = 0$), in order to treat the ideal $\beta = 1$ laser. Jin *et al.* also use Scully-Lamb laser theory, which adiabatically eliminates the atomic variables. This approach cannot address the λ dependence contained in the master equation (9).

A strong model dependence is actually to be expected in the cavity-QED limit. This is just one more indication of the failure of the laser laser–phase-transition analogy. Results obtained from conventional laser theories ($\beta \ll 1$) do not depend on the details of the model used, a consequence of the universality associated with phase transitions. But there is no phase transition in the cavity-QED limit; the usual threshold behavior is replaced by a gradual evolution—with increasing pump power—of a nonlinear noise process. It is to be expected that the properties of this noise process vary as details of the physical model are changed.

V. CONCLUSIONS

The analogy with a second-order phase transition captures the physics of the "turn on" of a conventional laser. We have discussed how the analogy is to be applied to cavity-QED lasers, in particular, to the ideal $\beta = 1$ laser. We have shown that β is the inverse of the saturation photon number n_{sat}. It follows that the cavity-QED limit, $\beta \to 1$, moves in the opposite direction to the "thermodynamic" limit, $n_{sat} = \beta^{-1} \to \infty$. One cannot therefore extrapolate the "thermodynamic" phase-transition analogy to the cavity-QED limit. A corollary to this result is that the ideal $\beta = 1$ laser is a *thresholdless* device. The definitions of a threshold which exist in the literature are arbitrary, and not grounded in an underlying phase-transition-like phenomenon.

Our discussion has been developed around an analysis of photon-number fluctuations. We showed how the Einstein rate equations used to model semiconductor cavity-QED lasers account partially for the fluctuations, but do not provide a full statistical treatment. As a simplest statistical model we introduced a birth-death master equation, constructed from a probabilistic interpretation of Einstein theory. We then characterized the photon-number fluctuations using the Fano factor which, for a conventional laser, reveals the enhanced threshold fluctuations of the order parameter (the complex field amplitude). We calculated the Fano factor by solving the birth-death master equation numerically. The results show clearly that the ideal $\beta = 1$ laser is a device without a threshold—a *thresholdless* device.

ACKNOWLEDGMENTS

The work of H.J.C. is supported by the National Science Foundation under Grant No. PHY-9214501. We wish to thank David Skinner for obtaining the numerical results displayed in Fig. 8.

[1] E. A. Hinds, in *Advances in Atomic, Molecular, and Optical Physics*, edited by D. Bates and B. Bederson (Academic Press, Boston, 1990), Vol. 28, pp. 237–289.
[2] *Cavity Quantum Electrodynamics*, edited by P. R. Berman (Academic Press, Boston, 1994).
[3] E. Purcell, Phys. Rev. **69**, 681 (1946).
[4] D. Kleppner, Phys. Rev. Lett. **47**, 233 (1981).
[5] E. Yablonovitch, Phys. Rev. Lett. **58**, 2059 (1987); S.

John, *ibid.* **58**, 2486 (1987).
[6] K. Drexhage, in *Progress in Optics*, edited by E. Wolf (North-Holland, Amsterdam, 1974), Vol. XII, pp. 163–232.
[7] D. J. Heinzen, J. J. Childs, J. E. Thomas, and M. S. Feld, Phys. Rev. Lett. **58**, 1320 (1987); F. DeMartini, G. Innocenti, G. R. Jacobovitz, and P. Mataloni, *ibid.* **59**, 2955 (1987); H. Yokoyama, M. Suzuki, and Y. Nambu, Appl. Phys. Lett. **58**, 2598 (1991).
[8] A. G. Vaidyanathan, W. Spencer, and D. Kleppner, Phys. Rev. Lett. **47**, 1592 (1981); G. Gabrielse and H. Dehmelt, *ibid.* **55**, 67 (1985); R. Hulet, E. Hiffer, and D. Kleppner, *ibid.* **55**, 2137 (1985)
[9] J. J. Sanchez-Mondragon, N. B. Narozhony, and J. H. Eberly Phys. Rev. Lett. **51**, 550 (1983); G. S. Agarwal, *ibid.* **53**, 1732 (1984); J. Opt. Soc. Am. B **2**, 480 (1985).
[10] Y. Kaluzny, P. Goy, M. Gross, J. N. Raimond, and S. Haroche, Phys. Rev. Lett. **51**, 1175 (1983); M. G. Raizen, R. J. Thompson, R. J. Brecha, H. J. Kimble, and H. J. Carmichael, *ibid.* **63**, 240 (1989); Y. Zhu, D. J. Gauthier, S. E. Morin, Q. Wu, H. J. Carmichael, and T. W. Mossberg, *ibid.* **64**, 2499 (1990).
[11] R. J. Thompson, G. Rempe, and H. J. Kimble, Phys. Rev. Lett. **68**, 1132 (1992).
[12] C. W. Gardiner, Phys. Rev. Lett. **56**, 1917 (1986).
[13] H. J. Carmichael, A. Lane, and D. F. Walls, J. Mod. Opt. **34**, 821 (1987); Phys. Rev. Lett. **58**, 2539 (1987).
[14] A. S. Parkins and C. W. Gardiner, Phys. Rev. A **40**, 3796 (1989); **42**, 5765(E) (1990).
[15] P. R. Rice and L. M. Pedrotti, J. Opt. Soc. Am. B **9**, 200 (1992).
[16] T. Kobayashi, T. Segawa, A. Morimoto, and T. Sueta (unpublished); T. Kobayashi, A. Morimoto, and T. Sueta (unpublished).
[17] H. Yokoyama and S. D. Brorson, J. Appl. Phys. **66**, 4801 (1988).
[18] H. Yokoyama, Science **256**, 66 (1992).
[19] Y. Yamamoto, S. Machida, and G. Björk, Phys. Rev. A **44**, 657 (1991).
[20] F. T. Arecchi, G. S. Rodari, and A. Sona, Phys. Lett. **25A**, 59 (1967); F. T. Arecchi, M. Giglio, and A. Sona, *ibid.* **25A**, 341 (1967).
[21] M. Lax and W. H. Louisell, IEEE J. Quantum Electron. **QE-3**, 47 (1967).
[22] H. Risken, in *Progress in Optics* (Ref. [6]), Vol. VIII, pp. 238–94.
[23] S. Singh and L. Mandel, J. Opt. Soc. Am. **72**, 304 (1982).
[24] S. L. McCall, A. F. J. Levi, R. E. Slusher, S. J. Pearton, and R. A. Logan, Appl. Phys. Lett. **60**, 289 (1992); R. E. Slusher, Opt. and Photon. News **4** (2), 8 (1993).
[25] D. Y. Chu and S. T. Ho, J. Opt. Soc. Am. B, **10**, 381 (1993).
[26] H. J. Kimble, in *Cavity Quantum Electrodynamics* (Ref. [2]), pp. 203–266. In the notation of this paper, β, for an optimally coupled atom, is given by $2C_1/(1+2C_1)$, $C_1 = g_0/2\gamma\kappa$. Bad-cavity conditions should be assumed so that irreversible spontaneous emission into the cavity mode takes place. Using the system parameters quoted in the caption to Fig. 15, for example, $\kappa/2\pi$ might be increased by a factor of 30 to obtain $\beta \approx 0.5$.
[27] S. E. Morin, C. C. Yu, and T. W. Mossberg, Phys. Rev. Lett. **73**, 1489 (1994).
[28] P. Goy, J. M. Raimond, M. Gross, and S. Haroche, Phys. Rev. Lett. **50**, 1903 (1983).
[29] S. Haroche and J. M. Raimond, in *Advances in Atomic and Molecular Physics*, edited by D. Bates and B. Bederson (Academic Press, Boston, 1985), Vol. 20, pp. 347–411.
[30] D. Meschede, H. Walther, and G. Müller, Phys. Rev. Lett. **54**, 551 (1985).
[31] G. Raithel, C. Wagner, H. Walther, L. M. Narducci, and M. O. Scully, in *Cavity Quantum Electrodynamics* (Ref. [26]), pp. 57–121.
[32] V. DeGiorgio and M. O. Scully, Phys. Rev. A **2**, 1170 (1970).
[33] R. Graham and H. Haken, Z. Phys. **237**, 31 (1970).
[34] S. Grossmann and P. H. Richter, Z. Phys. **242**, 458 (1971).
[35] F. DeMartini and G. R. Jacobovitz, Phys. Rev. Lett. **60**, 1711 (1988); F. DeMartini, F. Cairo, P. Mataloni, and F. Verezegnassi, Phys. Rev. A **46**, 4220 (1992).
[36] G. Björk and Y. Yamamoto, IEEE J. Quantum Electron. **QE-27** 2386 (1991).
[37] Y. Yamamoto, S. Machida, and G. Björk, Opt. Quantum Electron. **24**, S215 (1992).
[38] Y. Yamamoto and R. E. Slusher, Phys. Today **46** (6), **66** (1993).
[39] M. O. Scully and W. E. Lamb, Phys. Rev. Lett. **16**, 853 (1966); Phys. Rev. **159**, 208 (1967).
[40] M. Sargent III, M. O. Scully, and W. E. Lamb, Jr., *Laser Physics* (Addison-Wesley, Reading, MA, 1974), pp. 281–289.
[41] W. Weidlich, H. Risken, and H. Haken, Z. Phys. **201**, 396 (1967); Z. Phys. **204**, 223 (1967); H. Haken, H. Risken, and W. Weidlich, *ibid.* **206**, 355 (1967).
[42] R. Graham and H. Haken, Z. Phys. **234**, 193 (1970); **235**, 166 (1970).
[43] H. J. Carmichael, in *Lasers and Quantum Optics*, Proceedings of the International School on Lasers and Quantum Optics, Mar del Plata, Argentina, 22-31 August, 1988 (World Scientific, Singapore, 1990), pp. 52–85.
[44] Y. Mu and C. M. Savage, Phys. Rev. A **46**, 5944 (1992).
[45] W. E. Lamb, Jr., Phys. Rev. **134**, A1429 (1964); M. Borenstein and W. E. Lamb, Jr., Phys. Rev. A **5**, 1298 (1972).
[46] X. Wang, R. A. Linke, G. Devlin, and H. Yokoyama, Phys. Rev. A **47**, R2488 (1993).
[47] R. Jin, D. Boggavarapu, M. Sargent III, P. Meystre, H. M. Gibbs, and G. Khitrova, Phys. Rev. A **49**, 4038 (1994).
[48] P. R. Rice and H. J. Carmichael, IEEE J. Quantum Electron. **QE-24**, 1351 (1988).
[49] H. J. Carmichael, R. Brecha, and P. R. Rice, Opt. Commun. **82**, 73 (1991).
[50] C. M. Savage and H. J. Carmichael, IEEE J. Quantum Electron. **QE-24**, 1495 (1988).
[51] P. Alsing and H. J. Carmichael, Quantum Opt. **3**, 13 (1991).
[52] M. Wolinsky and H. J. Carmichael, Phys. Rev. Lett. **60**, 1836 (1988).
[53] These results appear in a number of references. We quote from Ref. [43] with the change of notation: $N_2 \to N$, $N_1 \to 0$, $\wp \to (\beta/\lambda)P = P/P_{thr}$, $n_{spon} \to (\beta/\lambda)P = P/P_{thr}$. In writing Eqs. (24b) and (26b) we have generalized the results in Ref. [43] by removing the restriction $\wp - 1 = P/P_{thr} - 1 \ll 1$.
[54] We are aware of one work in which measurements of the Fano factor for a conventional laser are reported: C.

Freed and H. A. Haus, Phys. Rev. **141**, 287 (1966). See Fig. 4, in particular, which displays the Fano factor for photocounts recorded outside the laser cavity over times long compared to the inverse bandwidth of the photon-number fluctuations. The Fano factor was recently measured for a microcavity laser by Jin *et al.* [47].

[55] A. W. Smith and J. A. Armstrong, Phys. Rev. Lett. **25**, 1169 (1966).

[56] F. Davidson and L. Mandel, Phys. Lett. A **25**, 700 (1967).

[57] M. Lax and M. Zwanziger, Phys. Rev. A **7**, 750 (1973).

[58] D. Meltzer, W. Davis, and L. Mandel, Appl. Phys. Lett. **17**, 242 (1970).

[59] Compare Fig. 5 with Fig. 5 in Ref. [43]. Note that the distributions which appear in Refs. [55,57,58] are not distributions of the number of photons inside the laser cavity, but distributions of the number of photocounts recorded over a short counting interval by a detector monitoring the laser output. The number of photocounts is not directly comparable, as an absolute number, with the photon number n in Fig. 5.

[60] D. Welford and A. Mooradian, Appl. Phys. Lett. **40**, 560 (1982).